J Electroceram (2009) 22:67–72
DOI 10.1007/s10832-008-9429-y

The effects of LSM coating on 444 stainless steel as SOFC interconnect

Hojune Hwang · Gyeong Man Choi

Received: 14 March 2007 / Accepted: 21 January 2008 / Published online: 5 February 2008

Abstract The effect of oxide ($La_{0.9}Sr_{0.1}MnO_3$, LSM) coating on the commercial stainless steel (STS444) interconnect as SOFC interconnect was examined by measuring the polarization resistance (R_p) of LSCF ($La_{0.6}Sr_{0.4}Co_{0.2}Fe_{0.8}$) cathodes of various electrolyte-supported cells ($La_{0.9}Sr_{0.1}Ga_{0.8}Mg_{0.2}$ [LSGM], $Ce_{0.9}Gd_{0.1}O_2$ [GDC10], or 8 mol% Y_2O_3-doped ZrO_2 [8YSZ]). The electrochemical impedance of LSCF cathodes was monitored during ~140 h in air at 600 and 700°C to determine the cathodic R_p values. With or without interconnect contacts, the magnitude of cathodic R_p value of LSGM electrolyte was similar to that of GDC electrolyte and much smaller than that of YSZ electrolyte. However, no apparent difference in the rate of increase was observed among the cathodes on the different electrolytes. Although the R_p value of the LSCF cathode in contact with LSM-coated STS444 was much reduced from that with uncoated STS444, the coating was not perfect to prevent the Cr evaporation from the interconnect and thus to avoid the degradation of LSCF cathode. Thus new coating methods or materials are needed to protect the LSCF cathode from the Cr poisoning.

Keywords Stainless steel · Interconnect · Cathode · Chromium · SOFC

1 Introduction

Metal interconnects are receiving much attention for the application in solid oxide fuel cells (SOFCs) at intermediate temperatures (600–800°C) due to their higher electrical conductivity, higher thermal conductivity, better ability to accommodate thermal stress, more reasonable mechanical strength, better easiness of fabrication, and most of all, lower cost than the ceramic interconnect. Various interconnect materials have specially been designed and tested for SOFCs such as chromium-based Ducrolly, nickel-based Haynes230 and Inconnel600, iron-based Crofer22, SUS430 and ZMG232 [1, 2]. However, when the metal interconnect is in contact with the SOFC cathode, the Cr in the interconnect alloy is known to poison the cathode and hence increase the polarization resistance (R_p) of cathode. The cathodic overpotential affected by the Cr poisoning varies, depending upon the electrode or the electrolyte materials [3]. The Cr_2O_3 formed near the interface of the zirconia electrolyte and the $La_{0.9}Sr_{0.1}MnO_3$ (LSM) cathode increases the Ohmic resistance and reduces the number of the triple-phase boundary sites [3, 4]. Since Cr was found on the surface of electrode particle instead of at the interface, $La_{0.6}Sr_{0.4}Co_{0.2}Fe_{0.8}O_3$ (LSCF) has been suggested as a more Cr-tolerant cathode than $La_{0.9}Sr_{0.1}MnO_3$ [3].

When the stainless-steel interconnect is exposed to a high temperature for a long time, the Cr from the stainless steel forms the resistive chromium-oxide layer on the surface and thus lowers the conductivity of the interconnect. The Cr also poisons the cathode and thus increases the cathodic overpotential. Many studies have focused on the ferritic Crofer22 due to its ability to form a conductive surface-layer composed of $(Mn,Cr)_3O_4$ spinel [5–7]. However, the thermally grown layer was not sufficiently good in maintaining the low area-specific resistance (ASR) [6, 8] and thus efforts have been made to enhance the conductivity of the oxide scale by coating the interconnect with the dense oxide-layers such as Mn-Co oxide [6, 7, 9] or Y-Co oxide [10]. When the Mn-Co-oxide spinel was coated on

H. Hwang · G. M. Choi (✉)
Fuel Cell Research Center and Department of Materials Science and Engineering, Pohang University of Science and Technology, Pohang 790-784, South Korea
e-mail: gmchoi@postech.ac.kr

STS430 or Crofer22, it lowered the thermal expansion mismatch and increased the electrical conductivity [11]. The multilayer and/or superlattice coatings of the stainless steel (304,440A) with Cr-Al-N also lowered the ASR [12]. In other report, it was shown that the La_2O_3 coating on the Crofer22 lowered the ASR [13].

In order to minimize the Cr effect on the cathode degradation, protective layers have been coated on the metallic interconnect to prevent the Cr vaporization. $La_{0.8}Sr_{0.2}FeO_3$ (LSF), sputter coated on Crofer22, improved the oxidation resistance and the electrical conductivity, but was considered ineffective in preventing the Cr diffusion [14]. When the surface of Crofer22 was treated with Ce, the oxidation resistance was decreased and the Cr migration into the cathode was reduced in short duration [15]. The $(Mn,Co)_3O_4$ spinel, thermally grown on the ferritic steel (Crofer22), lowered the ASR and it was also an effective barrier for the Cr migration [6, 7]. The Mn-Co-oxide spinel coated on STS430 and Crofer22 was shown to reduce the Cr vaporization [16, 17]. The Cr transport rate was also severely reduced by coating STS430 with $La_{0.65}Sr_{0.3}MnO_3$, $La_{0.6}Sr_{0.4}Co_{0.8}Fe_{0.2}O_3$, or $MnCo_2O_4$ [17]. There have also been approaches in designing the Cr-tolerant cathodes such as $LaNi_{0.6}Fe_{0.4}O_3$ (LNF) [18]. However, these attempts were still not good enough to ensure the low overpotential and the long-term operation. Therefore, more researches should be done on the protective coatings of interconnect that do not leak Cr, or cathodes that are not affected by the Cr.

In this study, we have chosen $La_{0.9}Sr_{0.1}MnO_3$ (LSM) as the coating material for the stainless-steel interconnects and examined the coating effect on the cathodic R_p. The Cr poisoning of $La_{0.6}Sr_{0.4}Co_{0.2}Fe_{0.8}O_3$ (LSCF) cathode was tested on three different electrolytes ($La_{0.9}Sr_{0.1}Ga_{0.8}Mg_{0.2}$ (LSGM), $Ce_{0.9}Gd_{0.1}O_2$ (GDC), or 8 mol% Y_2O_3-doped ZrO_2 (YSZ)). We have selected a commercial stainless-steel STS444 (POSCO, Korea) as an interconnect material which shows the highest electrical conductivity at SOFC operating temperatures among many commercial stainless-steels. STS444 has a merit in the low cost and has shown the ASR value which can be modified to match SOFC applications [19]. LSM was coated on STS444 by the high velocity oxy-fuel (HVOF) thermal-spray method. Thermal spray is an effective method in coating due to its many advantages including the low cost, the fast processing and the easiness in depositing patterns compared to other coating methods such as chemical vapor deposition or screen printing [20]. Since $La_{0.6}Sr_{0.4}Co_{0.2}Fe_{0.8}O_3$ (LSCF) is the most promising cathode material at an intermediate temperature in terms of low R_p and possibly tolerant of Cr poisoning, it was selected as a test cathode. Three different electrolytes were used to test the role of electrolytes (LSGM, GDC and YSZ) in determining the cathodic overpotential. In addition, we have compared the aerosol deposition method with the thermal spray method for depositing LSM-coating layer on STS444.

2 Experimental procedure

The uncoated and the LSM ($La_{0.9}Sr_{0.1}MnO_3$)-coated STS444 samples were obtained from RIST (Korea) and KIMM (Korea). The composition of STS444 (POSCO, Korea) was listed in Table 1 [19]. A thermal spray method was used by RIST (Korea) to produce the LSM coating layer with a thickness of ~40 μm. The LSM-coated STS444 by the aerosol deposition method was additionally prepared by KIMM (South Korea) for the comparison, with the coating thickness of ~10 and ~20 μm.

The electrolytes were prepared by the solid-state reaction process. La_2O_3 (99.99%, Strem Chemicals, USA), $SrCO_3$ (99.9%, High Purity Chemicals, Japan), Ga_2O_3 (99.9%, High Purity Chemicals) and MgO (99.9%, High Purity Chemicals) powders were used to form $La_{0.9}Sr_{0.1}Ga_{0.8}Mg_{0.2}$ (LSGM) using ball milling with zirconia balls for 12 h and calcined at 1200°C for 6 h. The powders were die-pressed and sintered at 1500°C for 6 h in air with the 3°C/min heating and cooling rates. YSZ (8 mol% Y_2O_3-doped ZrO_2, Tosho, Japan) powder was die-pressed and sintered at 1400°C for 3 h in air. CeO_2 (99.9%, High Purity Chemicals) and Gd_2O_3 (99.9%, High Purity Chemicals) powders were mixed to make $Ce_{0.9}Gd_{0.1}O_2$ (GDC) powder and ball-milled for 12 h. The calcined powder at 1200°C for 2 h was die-pressed followed by the cold-isostatic pressing at 200 MPa and sintering at 1650°C for 4 h.

LSGM, GDC and YSZ electrolytes were made into pellets (diameter ~18 mm, thickness ~1.2mm) and LSCF (Fuel Cell Materials) slurry was screen-printed with an area of 0.785 cm^2 on both sides of the electrolytes to minimize asymmetry in measuring the polarization resistance [21]. The electrolyte-supported cells with screen-printed cathodes were sintered at 1000°C/2 h for LSGM and GDC and at

Table 1 Chemical composition of commercial STS444 (POSCO, Korea).

STS444	Fe	C	Si	Mn	P	S	Cr	Ni	Mo	Cu	Al
wt%	bal.	0.006	0.26	0.24	0.02	0.001	18.59	0.21	1.96	0.04	0.048

900°C/2 h for YSZ, respectively. The lower firing temperature was used for YSZ than GDC or LSGM to minimize the possible $La_2Zr_2O_7$ formation. Pt paste (Engelhard No 6082, USA) and Pt mesh (Aldrich 52 mesh, USA) were used as a current collector, and also as a contact layer between the interconnect and the unit cell. The whole setup was heat-treated at 800°C in air for 1 h for the good contact. The impedance of specimens was measured at 600 and 700°C for ~140 h.

Figure 1 shows the schematic setup for the polarization measurement. The cathode in contact with the interconnect is a working electrode (W.E.) and the opposite electrode without the interconnect contact is a counter electrode (C.E.). A reference electrode (R.E.) is a point electrode located on the edge of the electrolyte. The working electrode monitors the change in the cathodic overpotential due to the contact with interconnects and the counter electrode measures that due to the change in the microstructure. With this configuration, we can measure the change in the cathodic polarization due to the particle sintering during the operation time and determine the net effect of the Cr poisoning.

The impedance of the cell in contact with the interconnect was measured with an impedance analyzer (SI1260 with SI 1287, Solatron, England). The sweeping frequency was 0.01 Hz–5 MHz with 0.1 V oscillation voltage. Microstructures were observed by a FE-SEM (JSM-6330F, JEOL, Japan).

3 Results and discussion

The microstructures of (a) the LSCF cathode on LSGM electrolyte and (b) the LSM-coated STS444 were shown in Fig. 2. The fine LSCF powders (diameter ~0.6μm) form a porous cathode and are in good contact with the electrolyte. The LSM coating on STS444 formed by a thermal spray method showed a dense structure which later turns out to be an effective layer to reduce the Cr evaporation. A ~40 μm-thick LSM layer was seen together with the top surface of the metal interconnect.

Figure 3 is the impedance pattern showing the effect of STS444 (with LSM coating) on the LSCF cathode of LSGM. The LSGM/LSCF/Pt mesh (Pt paste)//LSM-coated STS444 symmetric cell was maintained for ~140 h at 600°C, measuring the impedance of the total cell. A schematic diagram of the measurement configuration was shown in the figure. The lowest measurement frequency was 0.01 Hz, the peak at ~1 Hz, and the highest frequency was 5 MHz. The Ohmic resistance remained constant while the R_p increased with time. The Ohmic resistance measured at 600 and 700°C showed the negligible change during the experiment. Each impedance pattern was composed of two semicircles, one small and the other large. The larger one grew with time and thus may be associated with the Cr poisoning. The smaller semicircle remained nearly constant in the size. In many cases, the charge transfer resistance of

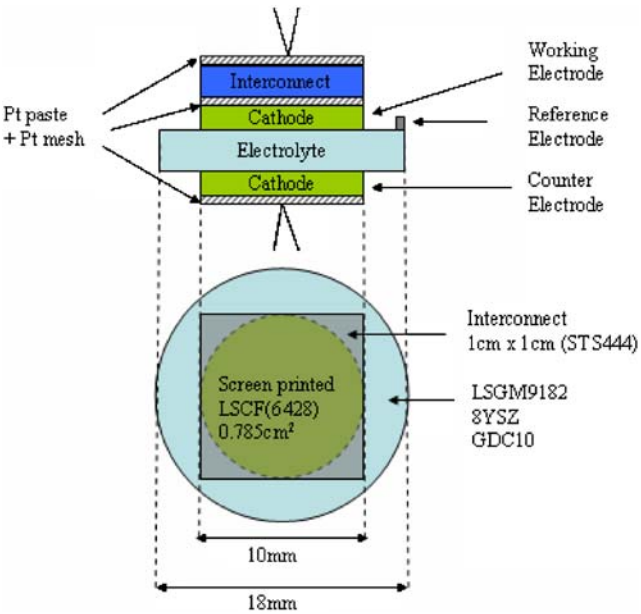

Fig. 1 A schematic of setup for the measurement of polarization resistance of symmetric cell. The working electrode is in contact with the interconnect and the counter electrode does not contact the interconnect. Pt paste and Pt mesh were inserted between the interconnect and the cathode for the good contact

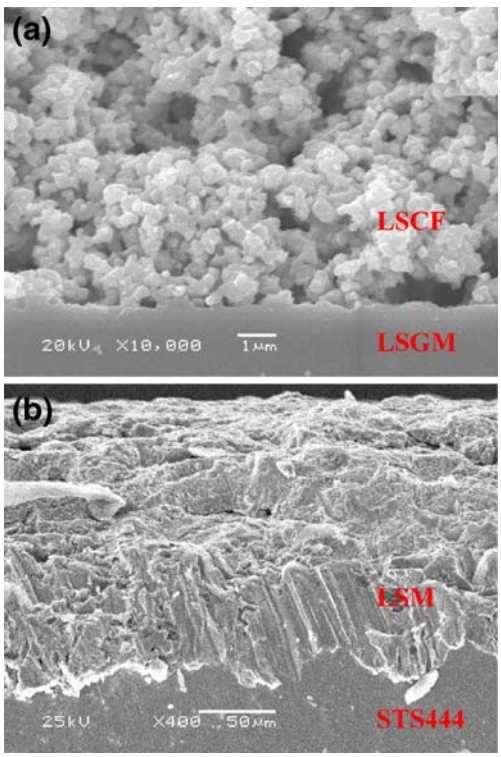

Fig. 2 Microstructure of (**a**) the LSCF cathode on LSGM electrolyte and (**b**) the LSM-coated STS444

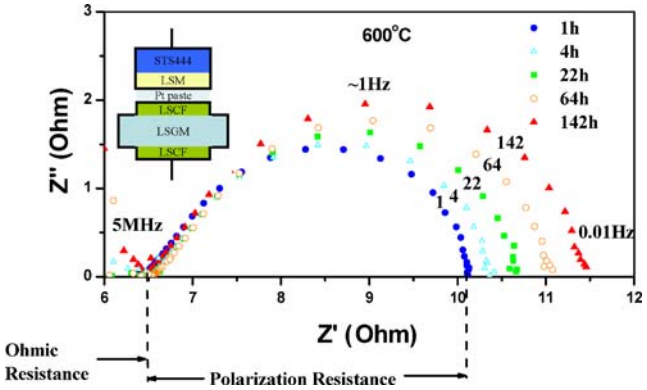

Fig. 3 Impedance patterns of the LSM-coated STS444 in contact with LSCF cathode on LSGM electrolyte, LSGM/LSCF/Pt paste (Pt mesh)/ LSM-coated STS444 symmetric cell, were measured at 600°C for 142 h. The semicircle increases in size with time

cathode is small and most resistance comes from either the slow diffusion or the slow adsorption. The Cr-poisoning effect was shown to be different, depending upon the electrode materials [3]. In the case of LSM cathode, Cr compounds mostly formed at the interface between the electrolyte and the cathode that limits the charge-transfer mechanism and decreases the number of triple phase boundary sites [3]. In the case of LSCF, Cr was found at the surface of cathode particles [3].

Figure 4 shows the impedance pattern of a GDC cell in contact with the metal interconnect. The counter electrode (C.E.) and the working electrode (W.E.) impedances were measured separately. Although not shown in this figure, YSZ or LSGM electrolytes showed the similar shapes. The LSCF cathode was screen-printed on the GDC electrolyte and was in contact with the LSM-coated STS444 at 600°C in air. The C.E. and the W.E. impedance values sum up to equal the total impedance. During the 116 h operation, the R_p of C.E. remained nearly unchanged. However, the W.E. shows a large increase in R_p even at 600°C, and this

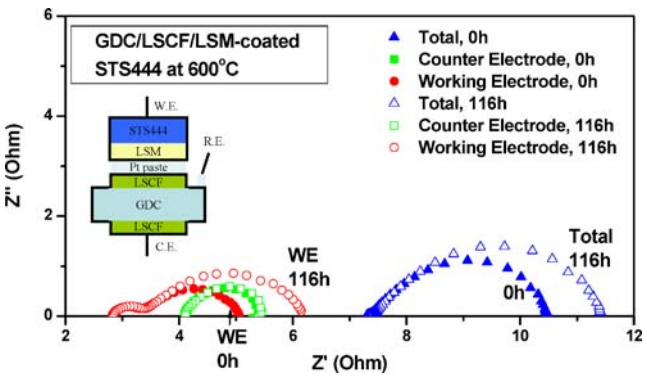

Fig. 4 The impedance patterns at 600°C of the total cell, the working electrode (W.E.), the counter electrode (C.E.) were separately measured and compared. The GDC cell with LSCF cathode was in contact with the LSM-coated STS444 and shown as an example. The total impedance is composed of the C.E. impedance and the W.E. impedance. The effect of Cr poisoning was only shown for the W.E.

increase mainly contributes to the increase in the total R_p. Thus we can safely assume that there was little particle sintering of the LSCF cathode for 116 h that increases the R_p. The impedance patterns of the C.E. showed that the impedance is composed of two semicircles that can not be easily separated. The similar impedance patterns were observed for the LSGM electrolyte in this study or in the literature data [22]. However, the impedance pattern for W.E. showed at least two easily separable semicircles. The appearance of larger semicircle at low frequency must be due to the Cr effect on the LSCF cathode. Thus the clear difference was shown between the electrodes with and without Cr exposure. The small difference in the Ohmic values for the W.E. and the C.E. sides of sample is due to the slight asymmetry of the reference electrode position.

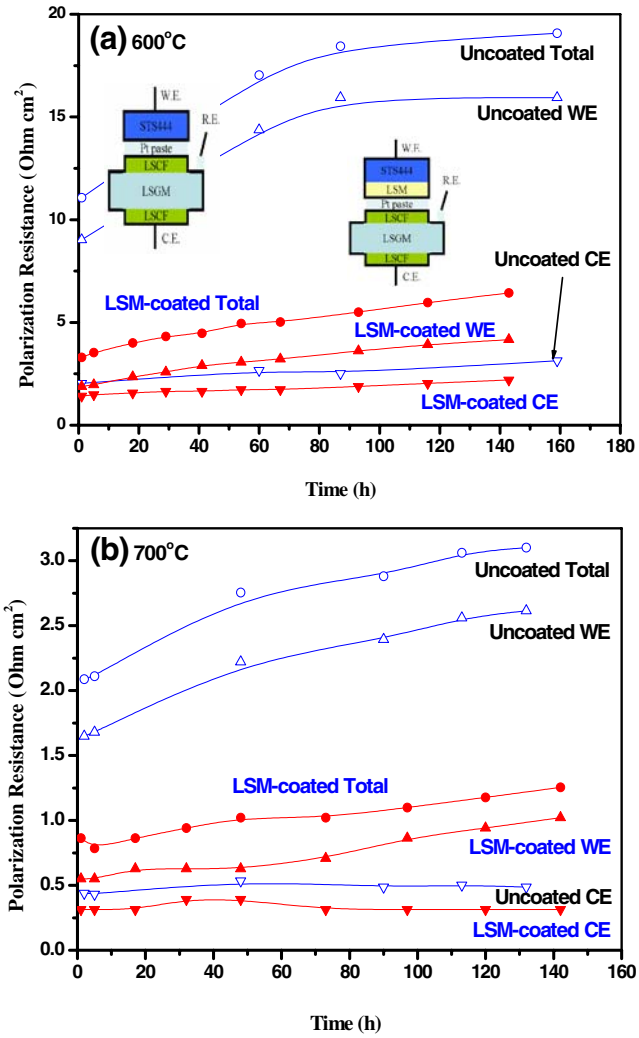

Fig. 5 The polarization resistance values of the total (W.E.+C.E.), the W.E., and the C.E. were separately plotted for the LSCF cathodes in contact with the uncoated or the LSM-coated STS444 interconnects at (**a**) 600°C and (**b**) 700°C with time. The polarization resistance of LSCF cathode was significantly reduced by coating the STS444 with LSM. The W.E. showed the higher R_p values than the C.E. at any time

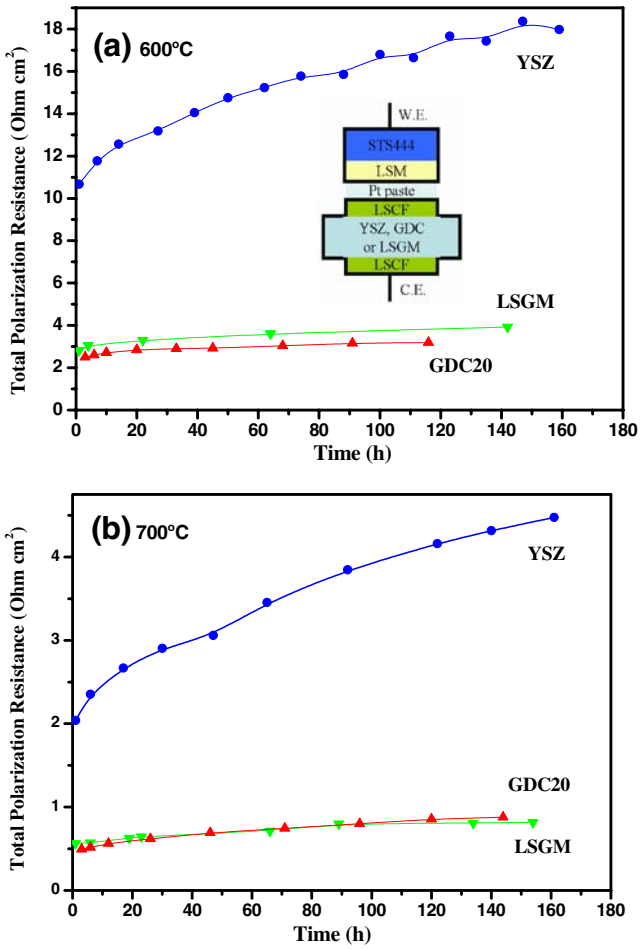

Fig. 6 The polarization resistance of LSCF cathode, in contact with the LSM-coated STS444, was compared for the YSZ, the LSGM and the GDC electrolytes at (**a**) 600°C and (**b**) 700°C with time

Figure 5 compares the R_p values of the LSCF cathodes that are in contact with the LSM-coated and the uncoated STS444. The specimen was heated for the good contact of the unit cell with the interconnect at 800°C/1 h. The measurements were performed at (a) 600°C for ~140 h and then subsequently at (b) 700°C for ~140 h. The coating effect of STS444 was clearly shown by the much smaller R_p value of the cell with the LSM-coated STS444 compared with the cell in contact with the bare STS444. The R_p values of the total and the working electrode decreased in a large amount due to the coating. The large R_p value was already shown after the 800°C/1 h bonding process. During the contact process, Cr may have already poisoned the cathode. Due to the LSM coating of the interconnect, the R_p value decreased from 19.1 to 3.9 Ω cm^2 after 142 h. Not only the R_p was smaller but the rate of R_p increase was also smaller with the LSM coating. The R_p value of LSCF with the uncoated STS444 increased by 72% after 142 h, while the R_p of the cathode with the coated STS increased by 39%. The R_p value of the counter electrode was always smaller that that of the working electrode. Thus Cr-poisoning effect was apparent for either the coated or the uncoated interconnects. However, the LSM-coating effect was evident, and this showed that the coating was essential when using STS444 as SOFC interconnect.

After observing the effectiveness of the LSM-coating on STS444 for LSGM electrolyte, we applied the coating to the systems with different electrolytes (YSZ and GDC). The total polarization resistance for the varying electrolytes with time at 600 and 700°C was shown in Fig. 6. The cathodic R_p value of the LSGM electrolyte was similar to that of the GDC and much smaller than that of the YSZ electrolytes. Matsuzaki and Yasuda showed the similar results; the LSM cathode on YSZ electrolyte showed a higher overvoltage than the LSM cathode on other electrolytes [3]. The R_p value in this study was also shown to follow the resistivity of the electrolyte material. The Ohmic resistivity of YSZ, LSGM and GDC at 600°C was measured as 124, 43, and 48 Ω cm, respectively. The proportionality between the R_p values and the electrolyte resistivities has been predicted and observed [23]. Although the R_p value was the largest for the LSCF cathode of YSZ electrolyte, no apparent difference in the rate of increase was noticeable among the LSCF cathodes of different electrolytes.

The coating thickness and coating method were altered to evaluate the coating effect. Figure 7 shows the R_p values of LSCF cathodes that are in contact with the ~10, ~20, ~40 μm-thick LSM coatings on STS444. The ~10, ~20 μm-thick layers were produced by the aerosol-deposition method and the ~40 μm-thick layer was produced by the thermal-spray method. Aerosol deposition method often produces the dense but thin layers at an

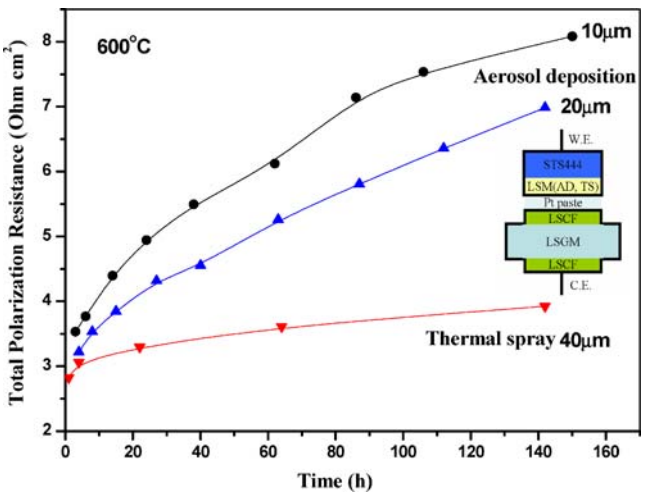

Fig. 7 The polarization resistance of LSCF cathodes in contact with two types of the LSM-coated STS444 was compared at 600°C. The aerosol deposition and the thermal spray methods were used for the LSM coatings

ambient temperature [24]. The total R_p increased with time. All LSM-coatings were not capable of stopping the increase in the cathode R_p with time. Although the starting R_p values were similar for all three coatings, 2.8–3.5 Ω cm^2, the ~10 μm LSM coating, fabricated by the aerosol-deposition method, resulted in the highest cathodic R_p value. The increase in the thickness from 10 to ~20 μm reduced the R_p by 10–20%, depending upon the time. The ~40 μm-thick LSM layer, fabricated by the thermal-spray method, was most effective to reduce the R_p value. The 700°C data showed the similar tendency. Thus the thickness alone was not the decisive factor for the prevention of Cr. The microstructure, the adherence, the surface finish or the density of the coating may need to be examined more in detail to clarify the difference. However, in the present study, the thermal spray was a more effective coating method than the aerosol deposition in the LSM coating on STS444.

Although the LSM coating reduced the Cr poisoning of LSCF cathode, no coating method was sufficiently good to prevent entirely the degradation of LSCF cathode on any electrolytes. Thus new coating methods or materials are needed to protect the LSCF cathode from the Cr poisoning. Alternatively, cathodes without strontium and manganese, such as $La(Ni,Fe)O_3$ or $(La,Ba)(Co,Fe)O_3$, have been suggested as the possible Cr-tolerant cathodes [18, 25].

4 Conclusions

The Cr poisoning effects of LSCF cathodes in contact with the STS444 interconnects have been successfully determined by comparing the cathodic polarization resistance (R_p) values of LSCF cathodes that are in contact with the interconnect with those that are not in contact with the interconnect. With or without the interconnect contacts, the magnitude of cathodic R_p value of LSGM electrolyte was similar to that of GDC electrolyte and much smaller than that of YSZ electrolyte. However, no apparent difference in the rate of increase was observed among the cathodes on the different electrolytes. Although the R_p values, measured at 600 and 700°C, of the LSCF cathodes in contact with the LSM-coated STS444 were much reduced from that in contact with the uncoated STS444, no coating methods were good enough to prevent entirely the Cr evaporation from the interconnect and thus to avoid the degradation of the LSCF cathodes. Thus new coating methods or materials are needed to protect the LSCF cathode from the Cr poisoning.

Acknowledgement This study was supported by Core Technology of Fuel Cell Program, MOCIE, Korea. RIST (Korea) provided the both LSM-coated and uncoated 444 stainless steel.

References

1. W.Z. Zhu, S.C. Deevi, Mater. Res. Bull. **38**, 957–972 (2003)
2. K. Fujita, T. Hashimoto, K. Ogasawara, H. Kameda, Y. Matsuzaki, T. Sakurai, J. Power Sources **131**, 270–277 (2004)
3. Y. Matsuzaki, I. Yasuda, J. Electrochem. Soc. **148**, A126–A131 (2001)
4. S.P. Jiang, J.P. Zhang, X.G. Zheng, J. Eur. Ceram. Soc. **22**, 361–373 (2002)
5. Z. Yang, J.S. Hardy, M.S. Walker, G. Xia, S.P. Simner, J.W. Stevenson, J. Electrochem. Soc. **151**(11), A1825–1831 (2004)
6. Z. Yang, G. Xia, J.W. Stevenson, Electrochem. Solid-State Lett. **8**, A168 (2005)
7. Z. Yang, G. Xia, S.P. Simner, J.W. Stevenson, J. Electrochem. Soc. **152**(9), A1896–1901 (2005)
8. S.P. Simner, M.D. Anderson, G.G. Xia, Z. Yang, L.R. Pederson, J.W. Stevenson, J. Electrochem. Soc. **152**(4), A740–A745 (2005)
9. X. Chen, P.Y. Hou, C.P. Jacobson, S.J. Visco, L.C. De Jonghe, Solid State Ion. **176**, 425–433 (2005)
10. W. Qu, L. Jian, D.G. Ivey, J.M. Hill, J. Power Sources **157**, 335–350 (2006)
11. X. Chen, P.Y. Hou, C.P. Jacobson, S.J. Visco, L.C. DeJonghe, Solid State Ion. **176**, 425–433 (2005)
12. P.E. Gannon, C.T. Tripp, A.K. Knospe, C.V. Ramana, M. Deibert, R.J. Smith, V.I. Gorokhovsky, V. Shutthanandan, D. Gelles, Surf. Coat. Technol. **188–189**, 55–61 (2004)
13. S. Fontana, R. Amendola, S. Chevalier, P. Piccardo, G. Caboche, M. Viviani, R. Molins, M. Sennour, J. Power Sources **171**, 652–662 (2007)
14. Z. Yang, G.G. Xia, G.D. Maupin, J.W. Stevenson, Surf. Coat. Technol. **201**, 4476–4483 (2006)
15. D.E. Alman, C.D. Johnson, W.K. Collins, P.D. Jablonski, J. Power Sources **168**, 351–355 (2007)
16. C. Collins, J. Lucas, T.L. Buchanan, M. Kopczyk, A. Kayani, P.E. Gannon, M.C. Deibert, R.J. Smith, D.S. Choi, V.I. Gorokhovsky, Surf. Coat. Technol. **201**, 4467–4470 (2006)
17. H. Kurokawa, C.P. Jacobson, L.C. DeJonghe, S.J. Visco, Solid State Ion. **178**, 287–296 (2007)
18. T. Komatsu, H. Arai, R. Chiba, K. Nozawa, M. Arakawa, K. Sato, Electrochem. Solid-State Lett. **9**, A9–A12 (2006)
19. D.H. Kim, J.H. Jun, S.G. Kim, J.H. Jun, Journal of the Korean Ceramic Society **42**, 833–841 (2005)
20. T. Degitz, K. Dobler, Weld. J. **81**, 50–52 (2002)
21. T. Kato, A. Momma, Y. Kaga, S. Nagata, Y. Kasuga, M. Kitase, Solid State Ion. **132**, 287–295 (2000)
22. K.B. Yoo, G.M. Choi, J. Eur. Ceram. Soc. **27**, 4211–4214 (2007)
23. T. Kenjo, Y. Kanehira, Solid State Ion. **148**, 1–14 (2002)
24. M. Nakada, H. Tsuda, K. Ohashi, J. Akedo, IEICE Trans. Electron. E90–C, 36–40 (2007)
25. Y.D. Zhen, S.P. Jiang, A.I.Y. Tok, ECS Transactions **7**, 263–269 (2007)